



# Acoustic properties of double-leaf membranes with a permeable leaf on sound incidence side

Sakagami, Kimihiro

Kiyama, Masakazu

Morimoto, Masayuki

---

(Citation)

Applied Acoustics, 63(8):911-926

(Issue Date)

2002-08

(Resource Type)

journal article

(Version)

Accepted Manuscript

(URL)

<https://hdl.handle.net/20.500.14094/90000366>



## **ACOUSTIC PROPERTIES OF DOUBLE-LEAF MEMBRANES WITH A PERMEABLE LEAF ON SOUND INCIDENCE SIDE**

**Kimihiro Sakagami\***

Environmental Acoustics Laboratory, Faculty of Engineering, Kobe University,  
Rokko, Nada, Kobe 657-8501 Japan

**Masakazu Kiyama**

Graduate School of Science and Technology, Kobe University, and NEA Ltd, Osaka, Japan

**and**

**Masayuki Morimoto**

Environmental Acoustics Laboratory, Faculty of Engineering, Kobe University,  
Rokko, Nada, Kobe 657-8501 Japan

\*Corresponding author:

Environmental Acoustics Laboratory, Faculty of Engineering, Kobe University,  
Rokko, Nada, Kobe 657-8501 Japan

Tel / Fax +81 78 803 6043

Email saka@kobe-u.ac.jp

## **ACOUSTIC PROPERTIES OF DOUBLE-LEAF MEMBRANES WITH A PERMEABLE LEAF ON SOUND INCIDENCE SIDE**

Kimihiro Sakagami , Masakazu Kiyama & Masayuki Morimoto

### **ABSTRACT**

The double-leaf membrane with a permeable leaf on its sound incidence side are usually used as roofs in actual membrane-structure buildings. They are modelled as of infinite extent, and their acoustic properties are theoretically analysed. The theory is experimentally validated. The permeability can significantly improve the sound absorption performance at high frequencies, and makes the characteristics similar to those of cavity-backed porous absorbents. At low frequencies the permeability also affects the sound absorption and insulation performance. At middle frequencies, the characteristics changed according to the permeability: a mass-spring peak appears if it is very high, and vanishes if lower. These effects are strongly dependent upon the mass of leaves, flow resistivity, cavity depth, etc. A detailed discussion is also given to shed some light on the mechanism of these effects.

## INTRODUCTION

Recent growth of membrane-structure buildings has made membranes widely used as a building material [1,2]. Membranes are usually used for the roofs and ceilings of the membrane-structure buildings. In some cases, they are also used in interior spaces. There have been reported some examples of the use of membrane materials for acoustic reflectors in multipurpose auditoria [3-5]. However, its most conventional use is a membrane-type absorber [6].

On the other hand, there have been some attempts to develop a new acoustical material with membranes. For example, Hashimoto et al. [7] proposed a membrane with additional weights to improve its sound insulation performance. To increase sound absorption, Koga [8] proposed a composite sheet-type material in which a thin film is sandwiched by two meshed metal sheets to increase energy loss in the material by introducing friction between the film and meshes.

In the case of the membrane-structure building, the greater part of the interior boundary is occupied by the membrane surface. This implies that the acoustics of the interior is governed mainly by the properties of the membrane [2]. Because the conventional membrane usually indicates little absorptivity [9], unless it has acoustical permeability, it often leads to poor acoustics in the interior. Therefore, the acoustic properties of the membrane should be adjusted.

Double-leaf membranes, which are often employed in the membrane-structure buildings, however, can be acoustically adjusted. The authors have shown that the conventional membrane-type absorption (membrane with a rigid backing and an air-cavity in-between) also occurs in the lightweight double-leaf membranes [10]. This property can be used to control the sound field of the interior.

An interior leaf of a double-leaf membrane is more or less permeable in many cases. Takahashi et al. [11] show that the permeability increases the membrane's absorptivity at high frequencies. The present authors explored the acoustic properties of a permeable membrane [12]. These studies suggest that the sound absorption performance of a double-leaf membrane should greatly be improved at middle-high frequencies by using a permeable interior leaf. This also suggests that a new-type lightweight acoustic panel can be used for interior partitions.

In this paper, the acoustic properties of a double-leaf membrane with a permeable leaf are theoretically analysed. An experiment is performed to validate the theory. A parametric study through some theoretical results is carried out to clarify the effect of parameters of the structure

on the acoustic properties. The absorption mechanism is also discussed in the light of numerical examples.

## ANALYSIS

Consider a double-leaf membrane consisting of two infinite membranes (Fig. 1) on which a plane wave  $p_i(x, z)$  impinges at the angle of incidence  $\theta$ . Only the first leaf (Leaf 1), at the incident side of the two membranes, has permeability characterised by its flow resistance  $Rh$ , which is the product of the flow resistivity  $R$  and the thickness  $h$  of the leaf. The surface density and tension of Leaf 1 and Leaf 2 are  $m_1, T_1$  and,  $m_2, T_2$ , respectively. The depth of the air cavity between the two leaves is  $d$ . The specific acoustic admittances of the Leaf 2 surfaces are  $A_3$  (incident side) and  $A_4$  (transmission side), respectively. The vibration displacements of the leaves are  $w_1(x)$  for Leaf 1 and  $w_2(x)$  for Leaf 2. The time factor is  $\exp(-i\omega t)$  ( $\omega$  angular frequency) which is suppressed throughout.

The pressure on the both side surfaces of Leaf 1 are denoted as  $p_1(x, z)$  (face: sound incident side) and  $p_2(x, z)$  (back: transmitted side), and those for Leaf 2 are  $p_3(x, z)$  (face) and  $p_4(x, z)$  (back). The pressure difference between Leaf 1's face and back surfaces is  $\Delta p$ .

For Leaf 1, from the definition of its flow resistance [13]:

$$Rh = \frac{\Delta p}{v_f - v}, \quad (1)$$

where  $v$  is the velocity of the material, and  $v_f$  is a velocity of the flow near and inside the material. Thus, the boundary condition on the either surfaces is:

$$\frac{\partial p_j}{\partial n} = i\rho_0 \omega v_f \quad (j=1,2), \quad (2)$$

where  $n$  is the outward normal of the boundary,  $\rho_0$  is the air density.

By a two-dimensional Helmholtz integral, the surface pressures,  $p_1(x, z)$  and  $p_2(x, z)$  are expressed, as follows [11]:

$$p_1(x, z) = 2p_i(x, 0) + \frac{i}{2} \int_{-\infty}^{\infty} [\rho_0 \omega^2 w_1(x_0) + ik_0 A_M \Delta p(x_0)] H_0^{(1)}(k_0 |x - x_0|) dx_0, \quad (3)$$

$$p_2(x, z) = \frac{-2i\rho_0 c_0 \omega w_2(x) \cos \theta + [i\rho_0 c_0 \omega w_1(x) - A_M \Delta p(x)] [(\cos \theta - A_3) e^{i\varphi} + (\cos \theta + A_3) e^{-i\varphi}]}{\cos \theta [(\cos \theta - A_3) e^{i\varphi} - (\cos \theta + A_3) e^{-i\varphi}]}, \quad (4)$$

where  $A_M = Rh/\rho_0 c_0$ .

For Leaf 2, the surface boundary pressure values,  $p_3(x, z)$  and  $p_4(x, z)$  are expressed by a two-dimensional Helmholtz integral as follows [8]:

$$p_3(x, z) = \frac{-i\rho_0 c_0 \omega w_2(x)(e^{i\varphi} + e^{-i\varphi}) + 2[i\rho_0 c_0 \omega w_1(x) - A_M \Delta p(x)]}{(\cos \theta - A_3)e^{i\varphi} - (\cos \theta + A_3)e^{-i\varphi}}, \quad (5)$$

$$p_4(x, z) = -\frac{i}{2} \int_{-\infty}^{\infty} [\rho_0 \omega^2 w_2(x_0) - ik_0 A_4 p_3(x_0, z)] H_0^{(1)}(k_0 |x - x_0|) dx_0, \quad (6)$$

where  $\varphi = k_0 d \cos \theta$ .

The force applied to the leaves equals to the pressure differences. The vibration displacements of Leaf 1 and 2,  $w_1(x)$  and  $w_2(x)$ , are described with the membranes' unit response,  $u_j(x)$  ( $j=1,2$ ),

$$w_1(x) = \int_{-\infty}^{\infty} \Delta p(\xi) u_1(x - \xi) d\xi, \quad (7)$$

$$w_2(x) = \int_{-\infty}^{\infty} [p_3(\xi, z) - p_4(\xi, z)] u_2(x - \xi) d\xi. \quad (8)$$

Using the Fourier transform technique, Eqs. (3)-(8) give the displacements of the leaves. The reflected and transmitted sound pressures,  $p_r$  and  $p_t$ , are obtained by the Helmholtz integral as follows [8]:

$$p_r(x, z) = \frac{N \cos \theta - A_M (M + N) + i\rho_0 c_0 \omega N \Gamma_1(k_0 \sin \theta) - 2i\rho_0 c_0 \omega A_M \Gamma_2(k_0 \sin \theta)}{N \cos \theta - A_M (M - N)} \times e^{ik_0(x \sin \theta - z \cos \theta)}, \quad (9)$$

$$p_t(x, z) = \frac{-i\rho_0 c_0 \omega}{\cos \theta + A_4} \Gamma_2(k_0 \sin \theta) e^{ik_0[x \sin \theta + (z-d) \cos \theta]}, \quad (10)$$

where  $B(k) = (k_0^2 - k^2)^{1/2}$ , and  $U_j(k) = [2\pi(T_j k^2 - m_j \omega^2)]^{-1}$  ( $j=1,2$ ) is the transformed unit response of the membranes, with

$$\Gamma_1(k) = \frac{R_1(k)\gamma_2(k) - R_2(k)\beta_2(k)}{\beta_1(k)\gamma_2(k) - \beta_2(k)\gamma_1(k)}, \quad (11)$$

$$\Gamma_2(k) = \frac{R_1(k)\gamma_1(k) - R_2(k)\beta_1(k)}{\beta_2(k)\gamma_1(k) - \beta_1(k)\gamma_2(k)}, \quad (12)$$

$$\beta_1(k) = Q(k) - 2\pi i \rho_0 c_0 \omega [k_0 N \cos \theta - B(k)M] U_1(k), \quad (13)$$

$$\beta_2(k) = -4\pi i \rho_0 c_0 \omega B(k) \cos \theta U_1(k), \quad (14)$$

$$\gamma_1(k) = 4\pi i \rho_0 c_0 \omega [B(k) + k_0 A_4] \{Q(k) - A_M [k_0 N \cos \theta - B(k)M]\} U_2(k), \quad (15)$$

$$\gamma_2(k) = -NQ(k)[B(k) + k_0 A_4] + 2\pi i \rho_0 c_0 \omega \{k_0 NQ(k) - 2\cos\theta Q(k)[B(k) + k_0 A_4] - 4A_M B(k)\cos\theta[B(k) + A_4]\}U_2(k), \quad (16)$$

$$R_1(k) = 4\pi B(k)N\cos\theta U_1(k), \quad (17)$$

$$R_2(k) = 8\pi A_M B(k)N\cos\theta[B(k) + k_0 A_4]U_2(k), \quad (18)$$

$$Q(k) = B(k)N\cos\theta + k_0 A_M N\cos\theta - B(k)MA_M, \quad (19)$$

$$M = (\cos\theta - A_3)e^{i\varphi} + (\cos\theta + A_3)e^{-i\varphi}, \quad (20)$$

and

$$N = (\cos\theta - A_3)e^{i\varphi} - (\cos\theta + A_3)e^{-i\varphi}. \quad (21)$$

As a pressure amplitude of unity is assumed for the incident plane wave, the oblique-incident sound absorption coefficient of the double-leaf is derived from Eq. (9) as:

$$\alpha = 1 - |p_r|^2, \quad (22)$$

and the transmission coefficient is obtained from Eq. (10) as:

$$\tau = |p_t|^2. \quad (23)$$

The sound reduction index is:

$$R = 10\log\left(\frac{1}{\tau}\right) = 20\log\left|\frac{1}{p_t}\right|. \quad (24)$$



## EXPERIMENTAL VALIDATION

### Procedure

To validate the theory, an experimental study was carried out and the results were compared with theoretical ones. In the experiment four types of double-leaf membrane with a permeable leaf on the incidence side were prepared. The details of the specimens are summarised in Table 1. All specimens were made of typical membrane materials for building purposes. As both the absorption and transmission coefficients need to be measured under identical condition, each specimen was installed in the aperture between coupled two reverberation chambers (See Fig. 2). The following assumptions involved in the theory were realised:

- (1) A double-leaf membrane of infinite extent divides the total space into two identical half spaces,
- (2) Sound energy in the source side can only be transmitted through the membrane.

Apart from the installation of the specimens, the measurements were carried out by conventional methods that are employed for the measurement of absorption and transmission in reverberation chambers. Five receiving points were used in both the source- and receiving-rooms in order to minimise the effect of poor diffuseness at low frequencies. Both the reverberation chambers had approximately the same volume ( $130 \text{ m}^3$ ) and surface area ( $153 \text{ m}^2$ ).

The tension of the leaves was not controlled, because it has a negligible effect on the acoustic properties [9-11].

### Results and comparison with theoretical results

Fig. 3 shows the measurement results of (a) absorption coefficient ( $\alpha$ ), (b) transmission coefficient ( $\tau$ ), and (c) their difference ( $\alpha - \tau$ ). The value of  $\alpha - \tau$  represents the energy actually dissipated in the structure. In Fig. 3, the calculated results for four types of double-leaf membranes used in the experiments are also shown. The specific acoustic admittances for the front and back surfaces of the impermeable Leaf 2 were previously measured [10] and include in the theoretical calculations. The admittances were measured in a tube with two microphones, and the specimens were tightly fixed to the rigid backing of the test tube [10]. The tension of the leaves,  $T = 1.0 \text{ N/m}$ , was assumed in the calculations. The field-incidence average (averaged over 0-78 degree of the angle of incidence) was employed to predict random incidence absorption and transmission coefficients from Eqs. (22) and (23), respectively.

Comparing the experimental results and the theoretical ones in Fig. 3, the following conclusions are obtained:

- (1) For  $\alpha$ ,  $\tau$  and  $\alpha-\tau$  in all cases shown in Fig. 3, the theoretical results are in fairly good agreement with the experimental values. Thus, the theory seems to be useful for predicting the acoustic properties of the double-leaf membrane.
- (2) The calculated peaks of  $\alpha$  and  $\alpha-\tau$  on the whole match those of experimental results: the shift between the experimental ones and theoretical ones is approximately 1/3 ... 2/3 octave. Peak frequency is caused by a deviation in the cavity depth of the experimental specimens from the designed value of 0.05 m:
- (3) Both the theoretical and measured values of  $\tau$  monotonically decrease with frequency, and tend to zero. There are some discrepancies at low frequencies; however, they are in good agreement at middle and high frequencies. Due to a low diffuseness of the reverberation chambers and the specimens' finite dimension, the theoretical and experimental results of  $\alpha$  show somewhat different behaviour at low frequencies.
- (4) When the flow resistance of the permeable Leaf 1 increases, the peak frequency in  $\alpha$  and  $\alpha-\tau$  is shifted towards low frequencies, and the peak value becomes lower. The value of  $\tau$ , however, does not change, even if the flow resistance changes.
- (5) The theoretical and experimental values of  $\alpha$ ,  $\tau$  and  $\alpha-\tau$  show the same tendency, when the surface density of Leaf 2 increases: at low frequencies,  $\alpha$  and  $\tau$  decrease as the surface density of Leaf 2 increases, however, they do not change at middle and high frequencies. The value of  $\alpha-\tau$  does not change at all in the whole frequency range, even if the mass of Leaf 2 changes. This means that the variation in  $\alpha$  due to change in the surface density of Leaf 2 is caused by a decrease in the transmitted energy.

Typical examples of the measured and calculated sound reduction index are shown in Fig. 4. The theoretical values are in fairly good agreement with the measured ones, especially at middle frequencies. Comparing two figures shown in Fig. 4, specimen No. 3, which has a permeable leaf with a flow resistance (0.158 kPa s/m) lower than No. 1 (3.300 kPa s/m), shows higher sound reduction index at middle and high frequencies. According to our previous results [12], the flow resistance around 1 kPa s/m maximises its internal energy loss. Therefore, the flow resistance of the permeable leaf in No. 1 is too much higher than the optimal value, resulting in the lower

sound reduction index, and that of No. 3 is rather closer to the optimal value to give the higher sound reduction index.

## PARAMETRIC STUDY

The field-incidence-averaged absorption and transmission coefficients,  $\alpha$  and  $\tau$ , are calculated from Eqs. (22) and (23). The difference  $\alpha-\tau$  is used to describe the actual energy loss occurring within the double-leaf membrane. In the following examples,  $\rho_0=1.2 \text{ kg/m}^3$ ,  $c_0=340 \text{ m/s}$  and  $h=0.05 \text{ m}$  are assumed throughout unless otherwise noted. Also  $T_1=T_2=1.0 \text{ N/m}$  is assumed throughout because the effects of the tension on the acoustic properties of membranes have been found negligible [9-11].

### Effects of Flow Resistance

The effect of the flow resistance (the product of the flow resistivity and the thickness of the leaf)  $Rh$  on  $\alpha-\tau$  is shown in Fig. 5. When  $Rh = \infty$ , a tendency similar to that of the conventional membrane-type absorber with a rigid back wall is seen, which is also similar to that of impermeable double-leaf membranes [10]. When  $10^2 \leq Rh \leq 10^4 \text{ Pa s/m}$ , the value of  $\alpha-\tau$  at high frequencies increases, making a plateau with slight fluctuations, typical of porous absorbents. The absorption reaches its maximum when  $Rh=10^3 \text{ Pa s/m}$ . This suggests an optimal value of  $Rh$  to maximise the value of  $\alpha-\tau$ , just as is the case for porous absorbents. As  $Rh$  decreases more and more, the characteristics approach those of an impermeable single membrane.

### Effects of Surface Density

Figs. 6 and 7 show the effect on  $\alpha-\tau$  of the surface density  $m_1$  (Leaf 1) and  $m_2$  (Leaf 2), respectively. At the frequency below the dip at mid-frequencies, the value of  $\alpha-\tau$  increases as  $m_1$  increases. The dip frequency does not vary with changes in  $m_1$ , but shifts to lower frequencies as  $m_2$  increases. At frequencies above 2 kHz, neither  $m_1$  nor  $m_2$  affects the value of  $\alpha-\tau$ .

### Effects of Cavity Depth

The effect of the cavity depth  $d$  on  $\alpha-\tau$  is shown in Fig 8. The characteristic fluctuates at mid-high frequencies as those of conventional porous materials. The peak value of  $\alpha-\tau$  observed near 3 kHz in the case of  $d=0.05 \text{ m}$ , moves to lower frequencies as  $d$  increases while its maximum value decreases.

### **Effects of Surface Acoustic Admittance**

The effects of the surface admittances of Leaf 2,  $A_3$  (face) and  $A_4$  (back), are shown in Figs. 9 and 10, respectively. The value of  $\alpha-\tau$  increases below 2 kHz as  $A_3$  increases. Increasing  $A_4$  makes slight increase in  $\alpha-\tau$  below 500 Hz, which is almost negligible, though.

## ABSORPTION MECHANISM

At low frequencies where  $d \ll \lambda$  ( $\lambda$ : acoustic wavelength) holds, the sound pressure within the air cavity is nearly constant and the effect of the cavity can be negligible. Therefore, the impedance of the entire system can be approximated by  $(1/Rh - 1/\omega m_1)^{-1} - i\omega m_2$ . Then the difference of the absorption and transmission coefficients for normal incidence,  $\alpha_n - \tau_n$ , becomes,

$$\alpha_n - \tau_n = \frac{4 \frac{\rho_0 c_0}{Rh}}{1 + 2 \frac{m_2}{m_1} + \left(\frac{m_2}{m_1}\right)^2 + \left(\frac{\omega m_2}{Rh}\right)^2 + 4 \left(\frac{\rho_0 c_0}{\omega m_1}\right)^2 + 4 \left(\frac{\rho_0 c_0}{Rh}\right)^2 + 4 \frac{\rho_0 c_0}{Rh}}. \quad (25)$$

This equation shows that  $\alpha_n - \tau_n$  increases as  $m_1$  increases, and decreases as  $m_2$  increases. When  $m_1 = \infty$ , Eq. (25) simplifies to the form,

$$\alpha_n - \tau_n = \frac{4 \frac{\rho_0 c_0}{Rh}}{1 + \left(\frac{\omega m_2}{Rh}\right)^2 + 4 \left(\frac{\rho_0 c_0}{Rh}\right)^2 + 4 \frac{\rho_0 c_0}{Rh}}. \quad (26)$$

At low frequencies,  $\omega m_2 / Rh \approx 0$ , and Eq. (26) agrees with  $\alpha_n - \tau_n$  calculated for the single-leaf permeable membrane of infinite mass. It means that, at low frequencies, the characteristics tend to those of a single-leaf permeable membrane, which are governed by  $Rh$  only, when  $m_1$  increases [12]. On the other hand, with increasing  $m_2$  the difference  $\alpha_n - \tau_n$  tends to zero.

Typical examples of  $\alpha - \tau$ , calculated from Eq. (22) averaged over the range of  $0-78^\circ$  of the angle of incidence (*i.e.*, ‘field-incidence’), for the following four extreme cases of the surface density are compared in Fig. 11:

- (1) A permeable single-leaf membrane of infinite mass,
- (2) A permeable double-leaf membrane of  $m_1 = m_2 = 1.0 \text{ kg/m}^2$ ,
- (3) A permeable double-leaf membrane of  $m_1 = \infty$ ,  $m_2 = 1.0 \text{ kg/m}^2$ ,
- (4) A permeable double-leaf membrane of  $m_1 = 1.0 \text{ kg/m}^2$ ,  $m_2 = \infty$ .

The characteristics of the permeable double-leaf with  $m_1 = \infty$  [case (3)] approach those of the permeable single-leaf of infinite mass [case (1)] as frequency decreases. This agrees with the result of the theoretical consideration using Eqs. (25) and (26), which neglect the effects of air-cavity. As frequency increases, the characteristics of the two cases (2) and (3), with the finite mass of Leaf 2 ( $m_2 = 1.0 \text{ kg/m}^2$ ) tend to be those of a double-leaf with the infinite mass of Leaf 2

( $m_2=\infty$ ), *i.e.*, those of a permeable membrane backed by an air layer with a rigid back wall, because the second leaf can hardly vibrate at high frequencies so that its characteristics tend to those of a rigid wall.

The middle frequency range can be considered as a transient stage from the low frequency characteristics to the high frequency characteristics: At low frequencies, the effect of the cavity disappears and the characteristics tend to be similar to those of a permeable single-leaf membrane, and at high frequencies Leaf 2 has an effect similar to a rigid-back wall so that the characteristics tend to be those of a permeable leaf with a rigid-back wall.

## CONCLUSIONS

In this paper the acoustic properties of a double-leaf membrane with a permeable leaf on its sound-incident side have been analysed. The theoretical results were found in good agreement with the experimental ones. The theory, therefore, seems to be useful for the prediction of the acoustic properties of a double-leaf membrane of this type. The effects of the parameters of the double-leaf membrane have been discussed in the light of theoretically calculated results. The sound absorption performance was evaluated by the difference of the absorption and transmission coefficients.

The permeability of the membrane improves the absorption performances in the high frequency range provided that the flow resistance of the membrane is suitably adjusted. At low frequencies, the sound absorption performance is improved when the mass of Leaf 1 increases, while it decreases when the mass of Leaf 2 increases. Both the masses are found to have no effect at higher frequencies than 2 kHz. The maximum of the fluctuation decreases and shifts to lower frequencies as the cavity depth increases. The sound absorption performance improves at lower frequencies if the acoustic admittance of the incident side surface of Leaf 2 increases, whereas that of the rear side has negligible effect.

The absorption mechanism of the permeable double-leaf membrane is also discussed. At low frequencies the characteristics are independent of air cavity. At high frequencies, they tend to those of a permeable membrane with an air back cavity and a rigid back wall.

## ACKNOWLEDGEMENTS

The authors are indebted to Professor Daiji Takahashi at Kyoto University for his valuable comments on this work. They also thank Toshiya Takada for his assistance in the numerical calculations, and Kaoru Kato for her assistance in the experimental study.



**Table 1.** Four types of double-leaf membrane used in experiment. The dimensions of all specimens are 2410 mm (height) and 2910 mm (width) and 50mm (cavity depth).

No	Leaf 1 (permeable)		Leaf 2 (impermeable)
	Surface density [ $\text{kg m}^{-2}$ ]	Flow resistance [ $\text{kPa s m}^{-1}$ ]	Surface density [ $\text{kg m}^{-2}$ ]
1	0.302	3.300	2.100
2	0.327	0.454	2.100
3	0.683	0.158	2.100
4	0.683	0.158	3.300

## REFERENCES

- [1] Maekawa Z. Acoustical design of the Kobe Port-Island Hall. In *Proceedings of the 12th ICA*, Vol. **II**, Toronto, Canada (1986) E3-6.
- [2] Sho D, Kageyama K, Kimura H, Hirata T, Onozuka K. Acoustic design of Tokyo Dome. *Trans. Committee of Architectural Acoustics, Acoust. Soc. Jpn.*, **AA88-15** (1988)(in Japanese).
- [3] Strøm S. Orchestra enclosures and stage design in multipurpose halls used for concerts. In *Proceedings of the 13<sup>th</sup> ICA*, Belgrade, Yugoslavia, 1989. pp. 183-186.
- [4] Asano A, Shimizu Y, Yabushita M, Kobayashi Y, Uchida S. On the flexible acoustic reflector made by complex rubber sheet. In *Reports of the autumn meeting of Acoust. Soc. Jpn.* **1-4-6** (1984) pp. 487-488. (in Japanese)
- [5] Kobayashi Y, Shioda M, Uchida S, Tokashiki K. Acoustical characteristics of flexible reflectors. In *Summaries of technical papers of annual meeting. Archi. Inst. Jpn.* **D** (1990) pp. 263-264. (in Japanese)
- [6] Brüel PV. Sound insulation and room acoustics. London: Chapman & Hall. 1951. Chap. 4.
- [7] Hashimoto N. Experimental study on sound insulation of membranes with small weights for application to membrane structures. *Applied Acoustics*, **48** (1996), pp. 71-84.
- [8] Koga S. Improvement of sound absorption of thin film - Studies of absorption characteristics by equivalent circuit. *J. Acoust. Soc. Jpn.(J)*, **52** (1996), pp. 92-98. (in Japanese)
- [9] Sakagami K, Morimoto M, Takahashi D. A note on the acoustic reflection of an infinite membrane. *Acustica*, **80** (1994), pp. 569-572.
- [10] Kiyama M, Sakagami K, Tanigawa M, Morimoto M. A basic study on acoustic properties of double-leaf membranes. *Applied Acoustics*, **54** (1) (1998) pp. 239-254.
- [11] Takahashi D, Sakagami K, Morimoto M. Acoustic properties of permeable membranes. *J. Acoust. Soc. Am.*, **99** (1996) pp. 3003-3009.
- [12] Sakagami K, Kiyama M, Morimoto M, Takahashi D. Detailed analysis of the acoustic properties of a permeable membrane. *Applied Acoustics*, **54** (2) (1998) pp. 93-111.
- [13] Pierce AD. Acoustics, an introduction to its physical principles and applications. New York: McGraw-Hill. 1981. (rpt. Acoust. Soc. Amer. 1989.) Sec. 3-8.

## LIST OF FIGURES

**Fig 1** Geometry of a permeable double-leaf membrane of infinite extent: the surface densities and tensions of the membranes are  $m_1$ ,  $T_1$  and  $m_2$ ,  $T_2$ , respectively. The flow resistance of Leaf 1 is  $Rh$ .  $A_3$  and  $A_4$  are the specific acoustic admittances of Leaf 2.

**Fig. 2** Block diagram of experimental arrangement.

**Fig. 3** Comparison of the theoretical (solid lines) and the experimental (dots) results: (a)  $\alpha$ , (b)  $\tau$  and (c)  $\alpha-\tau$ .

**Fig. 4** Examples of the theoretical (solid lines) and experimental (dots) results of sound reduction index for Specimen Nos.1 and 3 (See Table 1).

**Fig 5** Effect of the flow resistance of Leaf 1,  $Rh$ , on  $\alpha-\tau$ :  $Rh = 1$  (1),  $10^2$  (2),  $10^3$  (3),  $10^4$  (4),  $\infty$  (5)[Pa s/m] :  $m_1=m_2=1.0[\text{kg/m}^2]$ ,  $d = 0.05[\text{m}]$ ,  $A_3 = A_4 = 0.026$ , throughout.

**Fig 6** Effect of the surface density of Leaf 1,  $m_1$ , on  $\alpha-\tau$ :  $m_1 = 0.5$  (1),  $1.0$  (2),  $2.0$  (3),  $4.0$  (4) [ $\text{kg/m}^2$ ].  $Rh = 10^3[\text{Pa s/m}]$ ,  $m_2=1.0[\text{kg/m}^2]$ ,  $d=0.05[\text{m}]$ ,  $A_3 = A_4 = 0.026$ , throughout.

**Fig 7** Effect of the surface density of Leaf 2,  $m_2$ , on  $\alpha-\tau$ :  $m_2 = 0.5$  (1),  $1.0$  (2),  $2.0$  (3),  $4.0$  (4) [ $\text{kg/m}^2$ ].  $Rh = 10^3[\text{Pa s/m}]$ ,  $m_1=1.0[\text{kg/m}^2]$ ,  $d=0.05[\text{m}]$ ,  $A_3 = A_4 = 0.026$ , throughout.

**Fig 8** Effect of the cavity depth,  $d$ , on  $\alpha-\tau$ :  $d = 0.05$  (1),  $0.10$  (2),  $0.20$  (3),  $0.40$  (4)  $0.80$  (5) [m].  $Rh = 10^3$  [Pa s/m],  $m_1=m_2=1.0$  [ $\text{kg/m}^2$ ],  $A_3 = A_4 = 0.026$ , throughout.

**Fig 9** Effect of the specific acoustic admittance on the incident side of Leaf 2,  $A_3$ , on  $\alpha-\tau$ :  $A_3 = 0.013$  (1),  $0.026$  (2),  $0.056$  (3).  $Rh = 10^3$  [Pa s/m],  $m_1=m_2=1.0$  [ $\text{kg/m}^2$ ],  $d = 0.05$  [m],  $A_4 = 0.026$ , throughout.

**Fig 10** Effect of the acoustic specific admittance on the transmitted side of Leaf 2,  $A_4$ , on  $\alpha$ - $\tau$ :  $A_4 = 0.013$  (1),  $0.026$  (2),  $0.056$  (3).  $Rh = 10^3$  [Pa s/m],  $m_1=m_2=1.0$  [kg/m<sup>2</sup>],  $d = 0.05$  [m],  $A_3 = 0.026$ , throughout.

**Fig 11** Effect of the surface density of permeable membranes on  $\alpha$ - $\tau$ .  $Rh = 10^3$ [Pa s/m],  $d=0.05$ [m],  $A_3 = A_4 = 0.026$ , throughout.

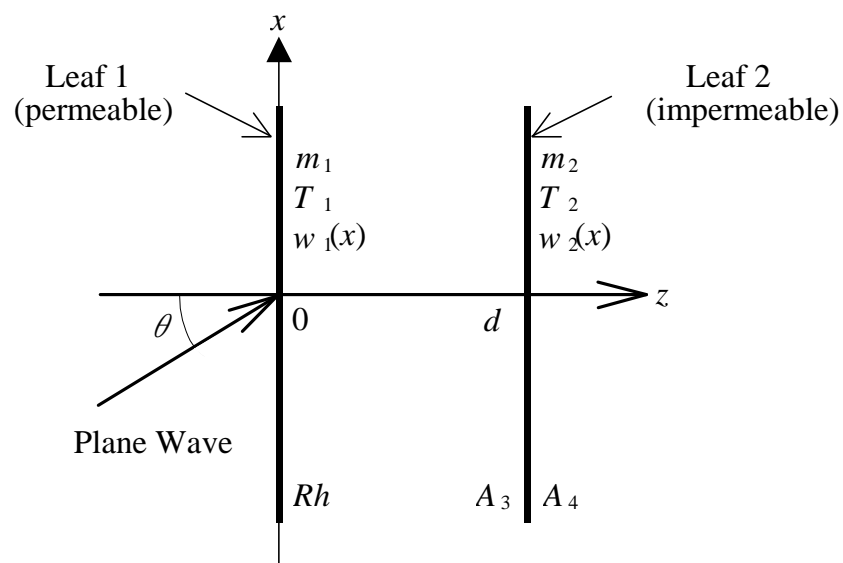


Fig 1 Geometry of a permeable double-leaf membrane of infinite extent: surface densities and tension of membranes are  $m_1$ ,  $T_1$  and  $m_2$ ,  $T_2$ . The flow resistance of Leaf 1 is  $Rh$ .  $A_3$  and  $A_4$  are the specific acoustic admittance of Leaf 2.

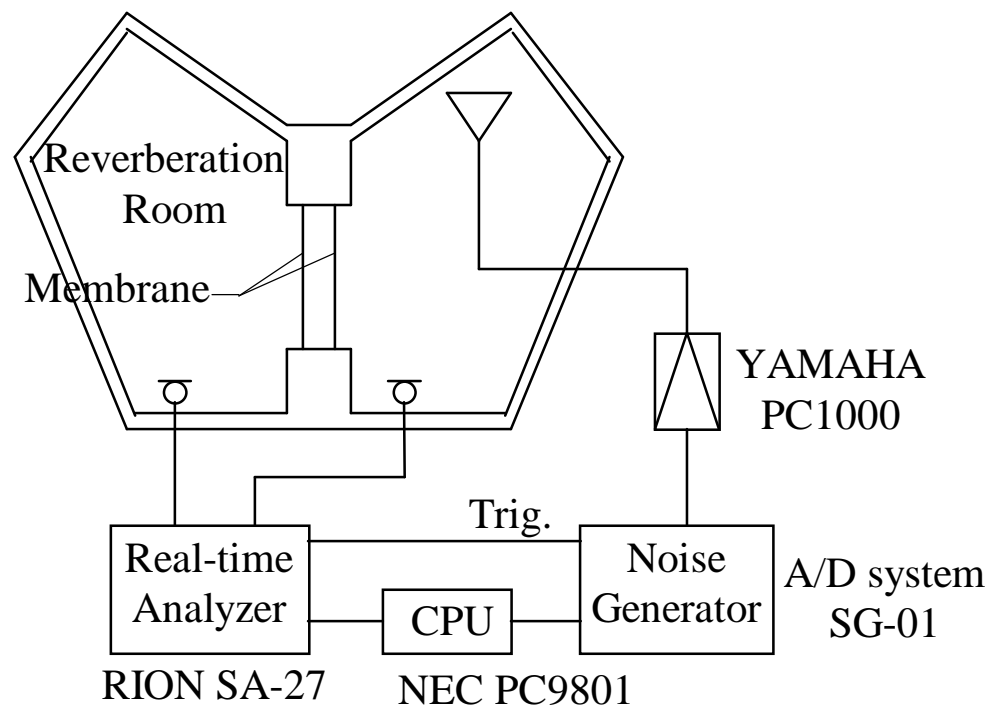
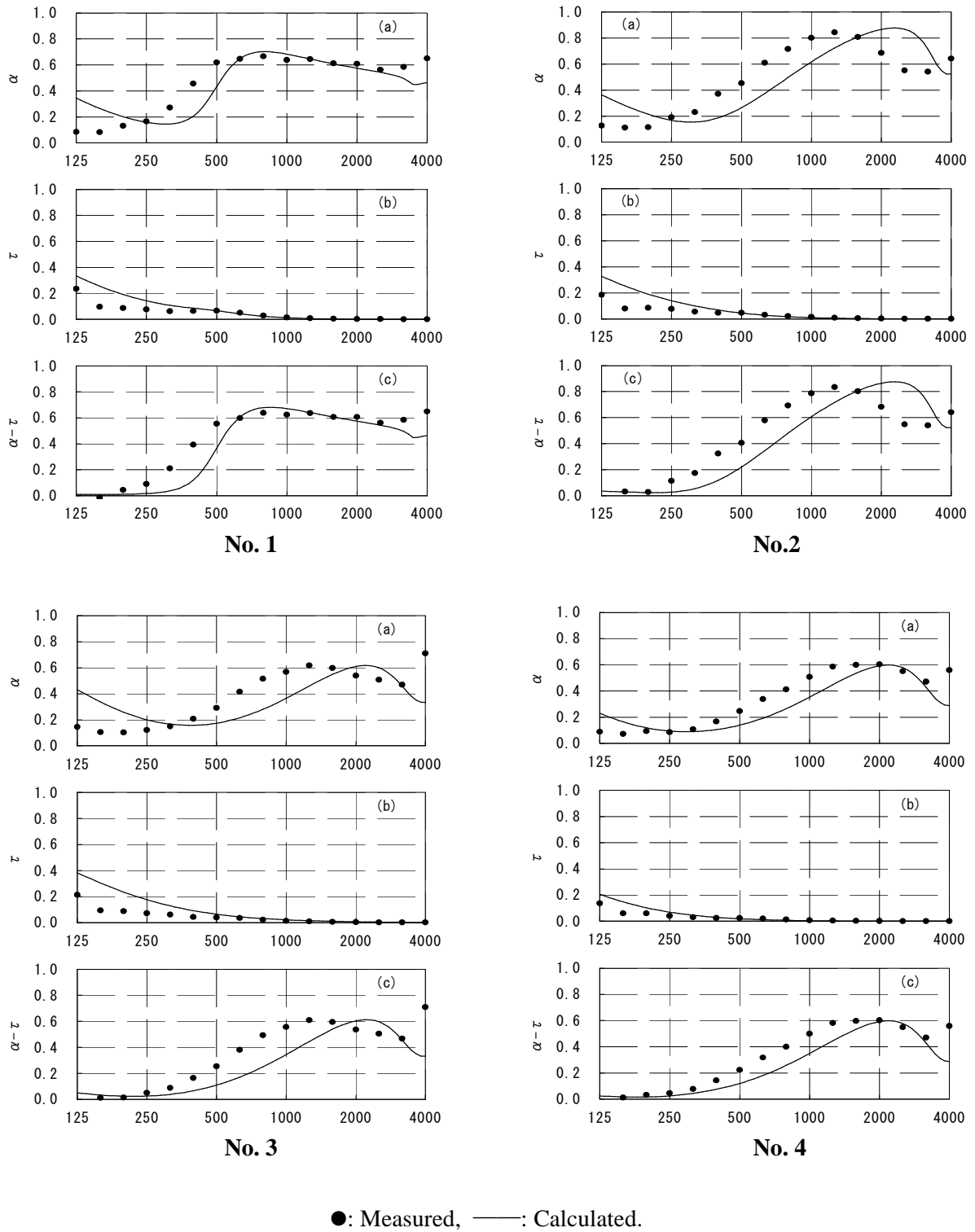


Fig. 2 Block diagram of experimental arrangement.

Fig. 3 Comparison of the theoretical (solid lines) and the experimental (dots) results: (a)  $\alpha$ , (b)  $\tau$ , and (c)  $\alpha - \tau$ .

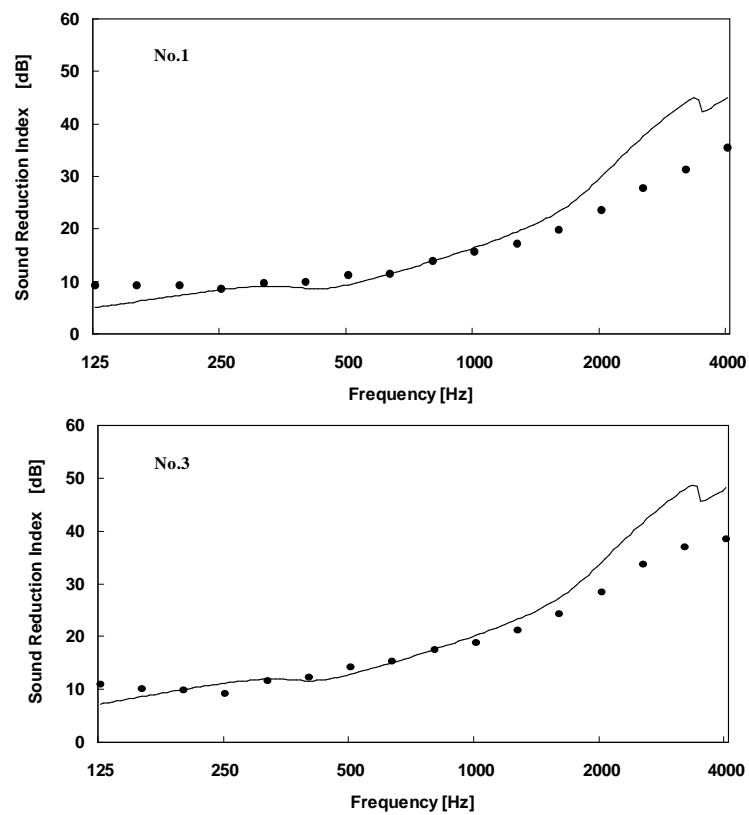


Fig. 4 Examples of the theoretical (solid lines) and experimental (dots) results of sound reduction index for Specimen Nos. 1 and 3 (See Table 1).



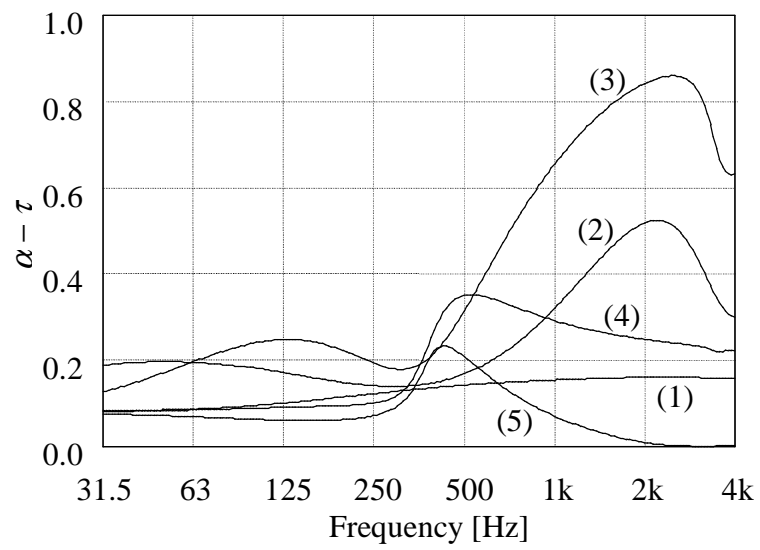


Fig 5 Effect of the flow resistance of Leaf 1,  $Rh$ , on  $\alpha-\tau$ :  $Rh = 1$  (1),  $10^2$  (2),  $10^3$  (3),  $10^4$  (4),  $\infty$  (5) [Pa s/m] :  
 $m_1=m_2=1.0$  [kg/m<sup>2</sup>],  $d=0.05$  [m],  $A_3=A_4=0.026$ , throughout.

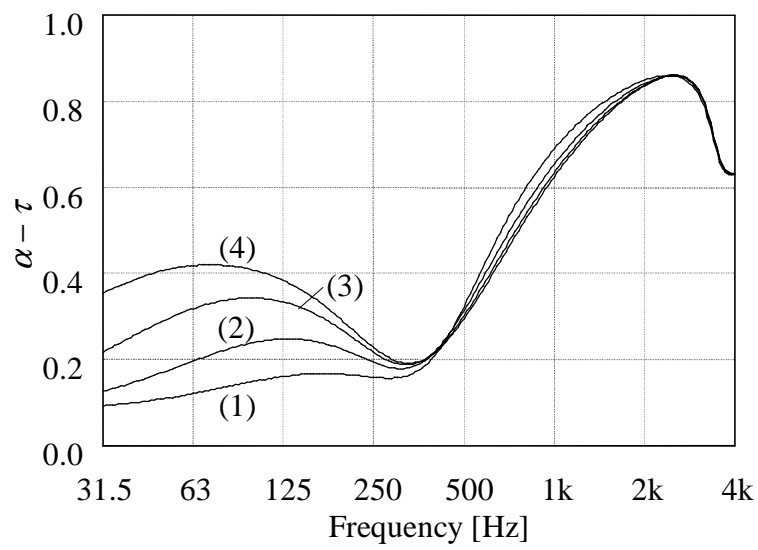


Fig 6 Effect of the surface density of Leaf 1,  $m_1$ , on  $\alpha-\tau$ :  $m_1=0.5$  (1), 1.0 (2), 2.0 (3), 4.0 (4) [ $\text{kg/m}^2$ ].  $Rh=10^3[\text{Pa s/m}]$ ,  $m_2=1.0[\text{kg/m}^2]$ ,  $d=0.05[\text{m}]$ ,  $A_3=A_4=0.026$ , throughout.

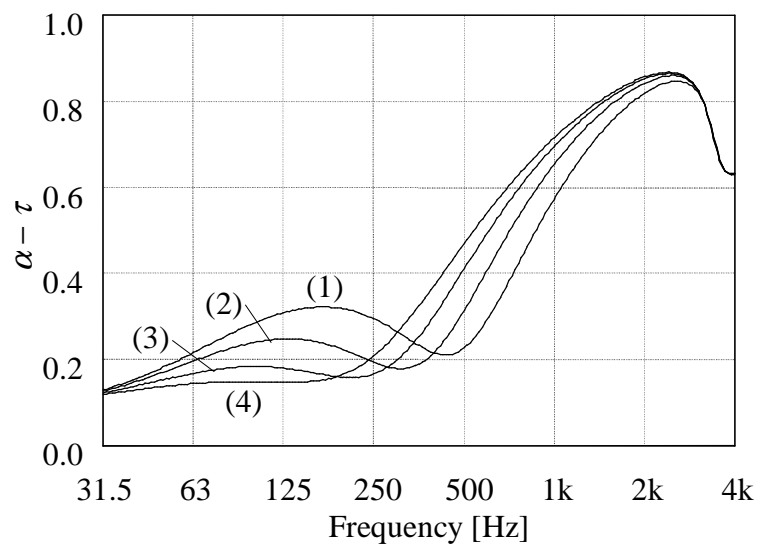


Fig 7 Effect of the surface density of Leaf 2,  $m_2$ , on  $\alpha - \tau$ :  $m_2 = 0.5$  (1), 1.0 (2), 2.0 (3), 4.0 (4) [kg/m<sup>2</sup>].  $Rh = 10^3$  [Pa s/m],  $m_1 = 1.0$  [kg/m<sup>2</sup>],  $d = 0.05$  [m],  $A_3 = A_4 = 0.026$ , throughout.

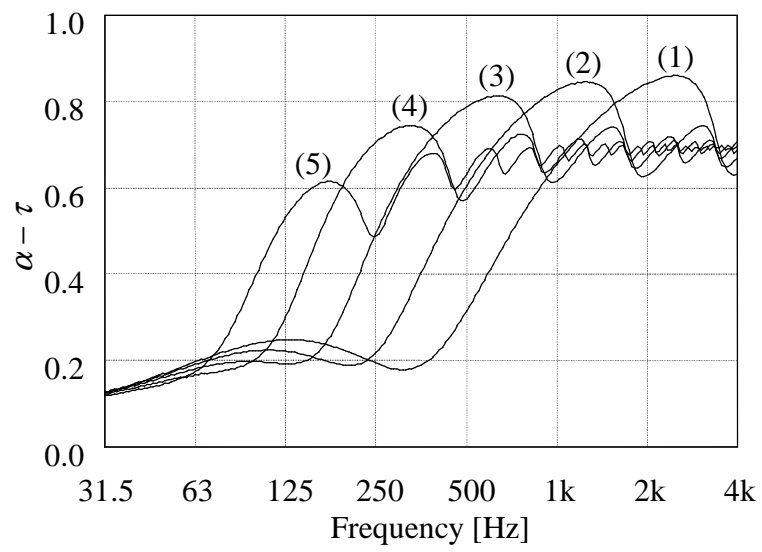


Fig 8 Effect of the cavity depth,  $d$ , on  $\alpha - \tau$ :  $d = 0.05$  (1),  $0.10$  (2),  $0.20$  (3),  $0.40$  (4)  $0.80$  (5) [m].  $Rh = 10^3$  [Pa s/m],  $m_1 = m_2 = 1.0$  [kg/m<sup>2</sup>],  $A_3 = A_4 = 0.026$ , throughout.

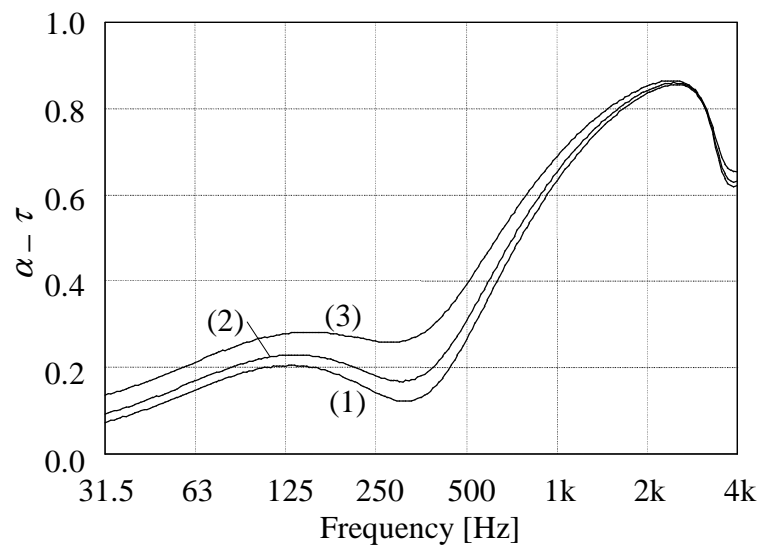


Fig 9 Effect of the acoustic specific admittance on the incident side of Leaf 2,  $A_3$ , on  $\alpha - \tau$ :  $A_3 = 0.013$  (1),  $0.026$  (2),  $0.056$  (3).  
 $Rh = 10^3$  [Pa s/m],  $m_1 = m_2 = 1.0$  [kg/m<sup>2</sup>],  $d = 0.05$  [m],  $A_4 = 0.026$ , throughout.

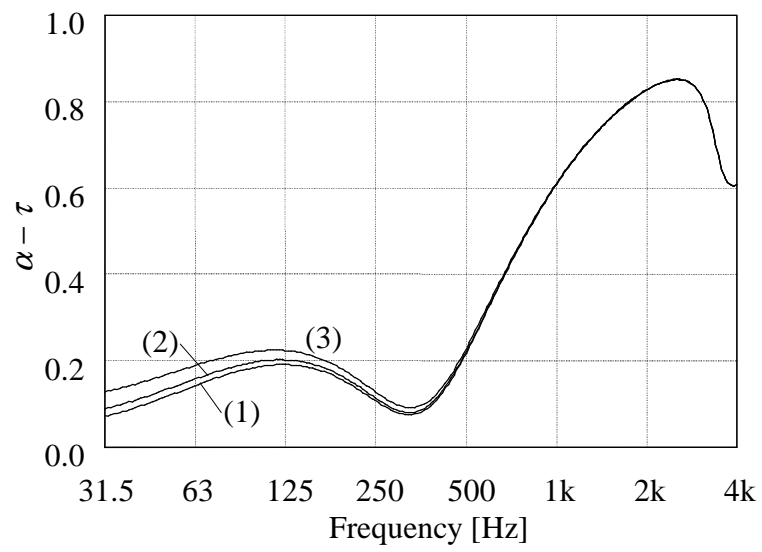


Fig 10 Effect of the specific acoustic admittance on the transmitted side of Leaf 2,  $A_4$ , on  $\alpha - \tau$ :  $A_4 = 0.013$  (1), 0.026 (2), 0.056 (3).  $Rh = 10^3$  [Pa s/m],  $m_1 = m_2 = 1.0$  [kg/m<sup>2</sup>],  $d = 0.05$  [m],  $A_3 = 0.026$ , throughout.

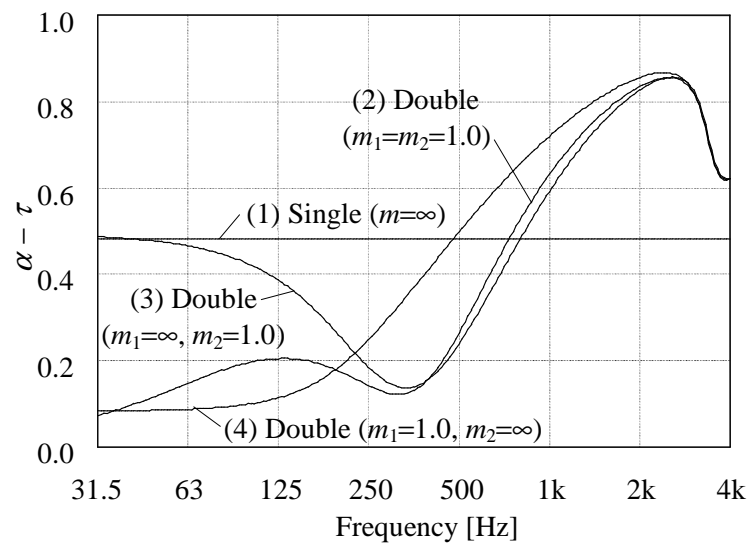


Fig 11 Effect of the surface density of permeable membranes on  $\alpha - \tau$ .  $Rh = 10^3$  [Pa s/m],  $d = 0.05$  [m],  $A_3 = A_4 = 0.026$ , throughout.